nature medicine

LETTERS

https://doi.org/10.1038/s41591-020-0910-8

Check for updates

Targeting CD70 with cusatuzumab eliminates acute myeloid leukemia stem cells in patients treated with hypomethylating agents

Carsten Riether[1,2]✉, Thomas Pabst[1], Sabine Höpner[1,2], Ulrike Bacher[3], Magdalena Hinterbrandner[1,2,4], Yara Banz[5], Rouven Müller[6], Markus G. Manz[6], Walid H. Gharib[7], David Francisco[7], Remy Bruggmann[7], Luc van Rompaey[8], Mahan Moshir[8], Tim Delahaye[8], Domenica Gandini[8], Ellen Erzeel[8], Anna Hultberg[8], Samson Fung[8,9], Hans de Haard[8], Nicolas Leupin[8] and Adrian F. Ochsenbein[1,2]✉

Acute myeloid leukemia (AML) is driven by leukemia stem cells (LSCs) that resist conventional chemotherapy and are the major cause of relapse[1,2]. Hypomethylating agents (HMAs) are the standard of care in the treatment of older or unfit patients with AML, but responses are modest and not durable[3–5]. Here we demonstrate that LSCs upregulate the tumor necrosis factor family ligand CD70 in response to HMA treatment resulting in increased CD70/CD27 signaling. Blocking CD70/CD27 signaling and targeting CD70-expressing LSCs with cusatuzumab, a human αCD70 monoclonal antibody with enhanced antibody-dependent cellular cytotoxicity activity, eliminated LSCs in vitro and in xenotransplantation experiments. Based on these preclinical results, we performed a phase 1/2 trial in previously untreated older patients with AML with a single dose of cusatuzumab monotherapy followed by a combination therapy with the HMA azacitidine (NCT03030612). We report results from the phase 1 dose escalation part of the clinical trial. Hematological responses in the 12 patients enrolled included 8 complete remission, 2 complete remission with incomplete blood count recovery and 2 partial remission with 4 patients achieving minimal residual disease negativity by flow cytometry at $<10^{-3}$. Median time to response was 3.3 months. Median progression-free survival was not reached yet at the time of the data cutoff. No dose-limiting toxicities were reported and the maximum tolerated dose of cusatuzumab was not reached. Importantly, cusatuzumab treatment substantially reduced LSCs and triggered gene signatures related to myeloid differentiation and apoptosis.

The tumor necrosis factor (TNF) receptor ligand CD70 is transiently upregulated on immune cells upon activation but is not expressed in normal tissue and on hematopoietic cells during homeostasis[6,7]. However, CD70 is expressed on various solid tumors and on non-Hodgkin lymphomas; its expression correlates with poor survival[8–10]. We recently demonstrated that $CD34^+$ AML cells (progenitors and LSCs) consistently express CD70 as well as its receptor CD27 and that cell-autonomous CD70/CD27 signaling propagates the disease[11]. The promoter of CD70 is sensitive to methylation[11,12]. To analyze whether HMA treatment results in upregulation of CD70 on LSCs, bone marrow $Lin^-CD90^-CD34^+CD38^-$ LSCs[1] from patients newly diagnosed with AML (Supplementary Table 1 and Supplementary Fig. 1a) were cultured in the presence and absence of a pharmacological concentration of decitabine or azacitidine[13,14]. HMA treatment reduced LSC numbers by approximately 45%, independent of the risk category[15] (Supplementary Fig. 1b). HMA-resistant LSCs had a significantly higher expression of CD70 than vehicle-treated control samples (Fig. 1a and Supplementary Fig. 1c,d). In contrast, HMA treatment reduced the numbers of $Lin^-CD90^-CD34^+CD38^+$ blasts and $Lin^-CD90^+CD34^+CD38^-$ hematopoietic stem cells (HSCs) from normal control bone marrow (Ctrl) without increasing CD70 expression (Fig. 1a and Supplementary Fig. 1b,d,e). Similarly, HMA treatment did not affect CD70 expression on natural killer (NK) cells and dendritic cells derived from the peripheral blood of healthy donors, two cell populations with reported transient CD70 expression during activation (Supplementary Fig. 1f,g) (ref. [7]).

HMA treatment increased CD70 expression on LSCs but not lymphocytes in the peripheral blood of patients with AML (Fig. 1b,c and Supplementary Fig. 1h). CD70 expression on AML LSCs correlated negatively with the degree of methylation of the CD70 promoter (Fig. 1d). In contrast, the CD70 promoter of HSCs showed only a moderate degree of methylation (Supplementary Fig. 1i). Treatment of $Lin^-CD90^-CD34^+$ AML cells in vitro with HMA significantly reduced the methylation of the CD70 promoter (Fig. 1e). The CD70 promoter contains binding sites for various transcription factors, such as specificity protein 1 (SP-1) (ref. [16]). *SP-1* expression was upregulated in $Lin^-CD90^-CD34^+$ AML cells after treatment with HMAs, whereas *miR-29b*, a negative regulator of *SP-1* (ref. [17]), was expressed at lower levels (Fig. 1f,g). Overall, these data indicate that HMAs induce CD70 expression in leukemia stem/progenitor cells (LSPCs) by demethylation of the CD70 promoter and by downregulating *miR-29b* levels, which results in the upregulation of the transcription factor SP-1.

Ligation of CD27 on LSCs by CD70 induces Wnt pathway activation, symmetric cell division and thereby maintains and

[1]Department of Medical Oncology, Inselspital, Bern University Hospital, University of Bern, Bern, Switzerland. [2]Department for BioMedical Research (DBMR), University of Bern, Bern, Switzerland. [3]Department of Hematology and Central Hematology Laboratory, Inselspital, Bern University Hospital, University of Bern, Bern, Switzerland. [4]Graduate School of Cellular and Biomedical Sciences, University of Bern, Bern, Switzerland. [5]Institute of Pathology, University of Bern, Bern, Switzerland. [6]Department of Medical Oncology and Hematology, University Hospital Zurich and University of Zurich, Zurich, Switzerland. [7]Interfaculty Bioinformatics Unit and SIB Swiss Institute of Bioinformatics, University of Bern, Bern, Switzerland. [8]argenx BVBA, Zwijnaarde, Belgium. [9]Fung Consulting Healthcare & Life Sciences, Eching, Germany. ✉e-mail: carsten.riether@insel.ch; adrian.ochsenbein@insel.ch

expands LSCs[11]. To determine the functional relevance of the HMA-induced upregulation of CD70 and increased CD70/CD27 signaling, we cultured LSCs in the presence of either a blocking αCD70 monoclonal antibody (mAb; clone 41D12-D)[18,19] or HMA alone or in combination (αCD70/HMA). 41D12-D is an αCD70 mAb with deficiency in effector function due to E233P/L234V/L235A amino acid substitutions in the CH2 region[18,19] and has the same binding domain as cusatuzumab. CD27 is shed from the cell surface after ligation with CD70 resulting in the release of soluble CD27 (sCD27) (ref. [7]). Treatment of LSCs with αCD70 mAb in vitro significantly reduced sCD27 levels suggesting that the CD70/CD27 interaction is efficiently blocked (Fig. 1h). HMA treatment of LSCs strongly increased sCD27 levels indicating enhanced CD70/CD27 signaling. This increased CD27 ligation and release of sCD27 was completely blocked by adding the αCD70 mAb (Fig. 1h). αCD70 treatment inhibited cell growth without affecting cell viability. In contrast, HMA treatment triggered cell death of LSCs (Supplementary Fig. 1j,k). Importantly, the αCD70/HMA combination treatment significantly reduced LSC numbers compared to monotherapy by increasing cell death (Supplementary Fig. 1j,k).

As reported previously[11], treatment with an αCD70 mAb reduced colony formation and induced differentiation of LSPCs as indicated by a trend toward increased cell numbers per colony (Fig. 1i and Supplementary Fig. 1l). The combination treatment synergistically reduced colony formation capacity compared to monotherapy (Fig. 1i). HMA treatment of LSCs before plating onto methylcellulose upregulated CD70 messenger RNA expression independent of the addition of αCD70 mAb (Supplementary Fig. 1m). The impaired colony formation after combination treatment observed after the first plating was maintained in subsequent replatings in the absence of αCD70 mAb and HMA (Fig. 1i). These experiments suggest that the αCD70/HMA combination strongly reduces LSCs in vitro. The clonogenic potential of HSCs was only affected to a minor extent by HMA treatment but not by the addition of the αCD70 mAb (Supplementary Fig. 1n); CD70 mRNA expression in HSCs was not affected by HMA treatment before plating onto methylcellulose (Supplementary Fig. 1o). These experiments indicated that blocking the CD70/CD27 interaction in combination with HMA treatment synergistically eliminates LSPCs in vitro.

To analyze the therapeutic potential of combining a blocking αCD70 mAb with HMAs in vivo, we performed patient-derived

Fig. 1 | αCD70/decitabine combination therapy eradicates human CD34$^+$CD38$^-$ LSCs in vitro and in vivo. a, 10^5 FACS-purified Lin$^-$CD90$^-$CD34$^+$CD38$^-$ LSCs from the bone marrow of patients newly diagnosed with AML and Lin$^-$CD90$^+$CD34$^+$CD38$^-$ HSCs from normal donor bone marrow (Ctrl; Supplementary Table 1) were cultured in StemSpan SFEM medium in the presence or absence of 0.5 μM of azacitidine (P8), decitabine (P11) or vehicle (Veh) in duplicates. Fold change delta mean fluorescence intensity (ΔMFI) CD70 after HMA treatment. AML is depicted as open symbols, Ctrl as closed symbols, azacitidine in red and decitabine in blue; $n=3$ and 16 patients with AML for azacitidine and decitabine, respectively; $n=3$ per HMA for Ctrl. Significance was determined using a two-sided Student's *t*-test (ALL versus Ctrl). **b**, Representative FACS plots of CD70 expression on Lin$^-$CD90$^-$CD34$^+$CD38$^-$ LSCs in the peripheral blood of a patient with AML (P22) at diagnosis and after 1 cycle of azacitidine treatment A(7), 75 mg m^{-2}, daily for 7 d. The isotype is depicted in gray; CD70 staining is shown in black at diagnosis and in red after treatment with azacitidine. ΔMFI: MFI staining—MFI isotype. The experiment was performed once for each patient shown. **c**, Fold change ΔMFI CD70 on Lin$^-$Cd90$^-$CD34$^+$CD38$^-$ AML LSCs and lymphocytes (decitabine, 20 mg kg^{-1}, daily for 5 d (D(5)) versus diagnosis; A(7) versus diagnosis. AML is depicted as open symbols, azacitidine in red and decitabine in blue; $n=3$ and 6 patients with AML for azacitidine and decitabine, respectively.) Significance was determined using a two-sided paired *t*-test. **d**, Correlation of methylation state at the SP-1 binding site of the CD70 promoter in Lin$^-$CD90$^-$CD34$^+$CD38$^-$ AML LSCs versus CD70 protein expression (ΔMFI CD70) in patients newly diagnosed with AML ($n=10$). The correlation coefficient *r* was determined using Pearson correlation. Significance was determined using a two-sided *t*-test. **e**–**g**, Lin$^-$CD90$^-$CD34$^+$ AML cells were cultured in the presence of the HMA decitabine (**e**) and decitabine or azacitidine (**f**,**g**) in triplicate as described in **a**. **e**, Methylation state of the CD70 promoter ($n=5$ patients with AML). SP-1 (**f**) and *miR-29b* (**g**) expression was assessed 48 h later ($n=3$ and 6 patients with AML for azacitidine and decitabine, respectively). Fold change is indicated as azacitidine versus vehicle or decitabine versus vehicle. Significance in **e** was determined using a two-sided paired *t*-test. The significance for **f**,**g** was determined using a two-sided one-sample test (hypothetical value = 1). **f**, fav: $P=0.01303$, int: $P=0.0079$ and adv: $P=0.0205$. **g**, fav: $P=0.0133$, int: $P=0.0178$, adv: $P=0.0127$. **h**,**i**, FACS-purified Lin$^-$CD90$^-$CD34$^+$CD38$^-$ LSCs from the bone marrow of patients newly diagnosed with AML were cultured in the presence or absence of 0.5 μM of HMA (AML is shown as open symbols, azacitidine in red and decitabine in blue) or αCD70 mAb (αCD70, clone 41D12-D, 10 μg ml^{-1}) alone or in combination in triplicates for 72 h (**h**) or overnight followed by plating onto methylcellulose containing αCD70 and HMA or both. Colonies and cells were enumerated after 14 d and replated in triplicates in the absence of treatment compounds (**i**). Sterile DMSO and a Ctrl mAb specific for the F protein of respiratory syncytial virus (palivizumab) were used as the mock treatment. **h**, sCD27 levels in supernatants ($n=3$ patients with AML each for azacitidine and decitabine). **i**, Serial replating experiments for AML LSCs. Data were normalized to vehicle control for each plating ($n=3$ and 5 patients with AML for azacitidine and decitabine, respectively). **h**,**i**, Significance was determined using one-way ANOVAs followed by Tukey's multiple comparison test. **j**–**o**, 5×10^6 FACS-purified CD45^{dim}SSC^{lo} cells from the bone marrow of patients newly diagnosed with AML (patients P10 and P25; Supplementary Table 1) were injected intravenously into the tail vein of sublethally irradiated (2.75 Gy) NSG mice. After engraftment (day 32 (P10) and day 97 (P25) after transplantation), mice were randomized to treatment with control mAb, 10 mg kg^{-1} αCD70 mAb (41D12-D) intraperitoneally (total of 3 injections) or decitabine (1.5 mg kg^{-1} per day) for five consecutive days[27] alone or in combination (P10, $n=2$ mice per group; P25, $n=4$ mice per group). One day after the last treatment, animals were killed and blood, spleen and bone marrow were analyzed. **j**, CD70 expression on huCD45$^+$lin$^-$CD34$^+$CD38$^-$ LSCs. Decitabine treatment is shown in blue and vehicle treatment in black. The solid lines represent CD70 staining and the dashed lines isotype control staining on LSCs. Significance was determined using a two-sided Student's *t*-test for P25 ($P=0.0015$). **k**, sCD27 levels in the sera of AML PDX mice. Significance for P25 was determined using a one-way ANOVAs followed by Tukey's multiple comparison test. **l**, Absolute numbers of huCD45$^+$lin$^-$CD34$^+$AML cells in the bone marrow. Significance for P25 was determined using a one-way ANOVA followed by Tukey's multiple comparison test. **m**, Frequency of CD38$^-$ AML LSCs within huCD45$^+$lin$^-$CD34$^+$ AML cells. Significance for P25 was determined using a one-way ANOVA followed by Tukey's multiple comparison test. **n**, Human colonies per 10^5 plated bone marrow cells from xenografted AML mice. Significance for P25 was determined using a one-way ANOVA followed by Tukey's multiple comparison test. **o**, LSC frequencies estimated using ELDA. Whole bone marrow cells at different dilutions (10^6, 5×10^5 and 10^5; Supplementary Table 1) from treated primary AML xenografted mice were transplanted into sublethally irradiated (2.75 Gy) secondary recipients. The engraftment frequencies of human AML cells in mouse bone marrow were assessed 67 (P10) and 82 (P25) days later. A frequency of >0.1% of human cells (huCD45$^+$CD33$^+$) in the murine bone marrow was rated as positive engraftment[1,28]. LSC frequencies were estimated with the ELDA software (http://bioinf.wehi.edu.au/software/elda/) (see Supplementary Table 2) and significant differences in LSC frequencies were calculated by chi-squared test (for P25: Veh versus αCD70/decitabine: $P=1.23\times10^{-5}$; decitabine versus αCD70/decitabine: $P=0.0037$; αCD70 versus CD70/decitabine: $P=0.0167$). Data are represented as the mean. Only statistically significant differences are indicated.

xenograft (PDX) experiments[1]. After engraftment of human AML cells, NOD/SCID/γc$^{-/-}$ (NSG) mice were randomized to treatment with vehicle (Veh), αCD70 mAb (3 × 10 mg kg^{-1} over 5 d), decitabine (1.5 mg kg^{-1} per day) or αCD70 mAb and decitabine in combination (Supplementary Fig. 2a). Decitabine treatment induced a significant upregulation of CD70 on LSCs but not on blasts (Fig. 1j and Supplementary Fig. 2b–d). Furthermore, sCD27 levels were elevated in the sera of PDX AML mice treated with decitabine compared to controls, indicating that decitabine-induced CD70 expression triggers CD70/CD27 signaling in AML mice in vivo (Fig. 1k). Treatment with the αCD70 mAb significantly reduced sCD27 levels especially in αCD70/decitabine-treated mice (Fig. 1k).

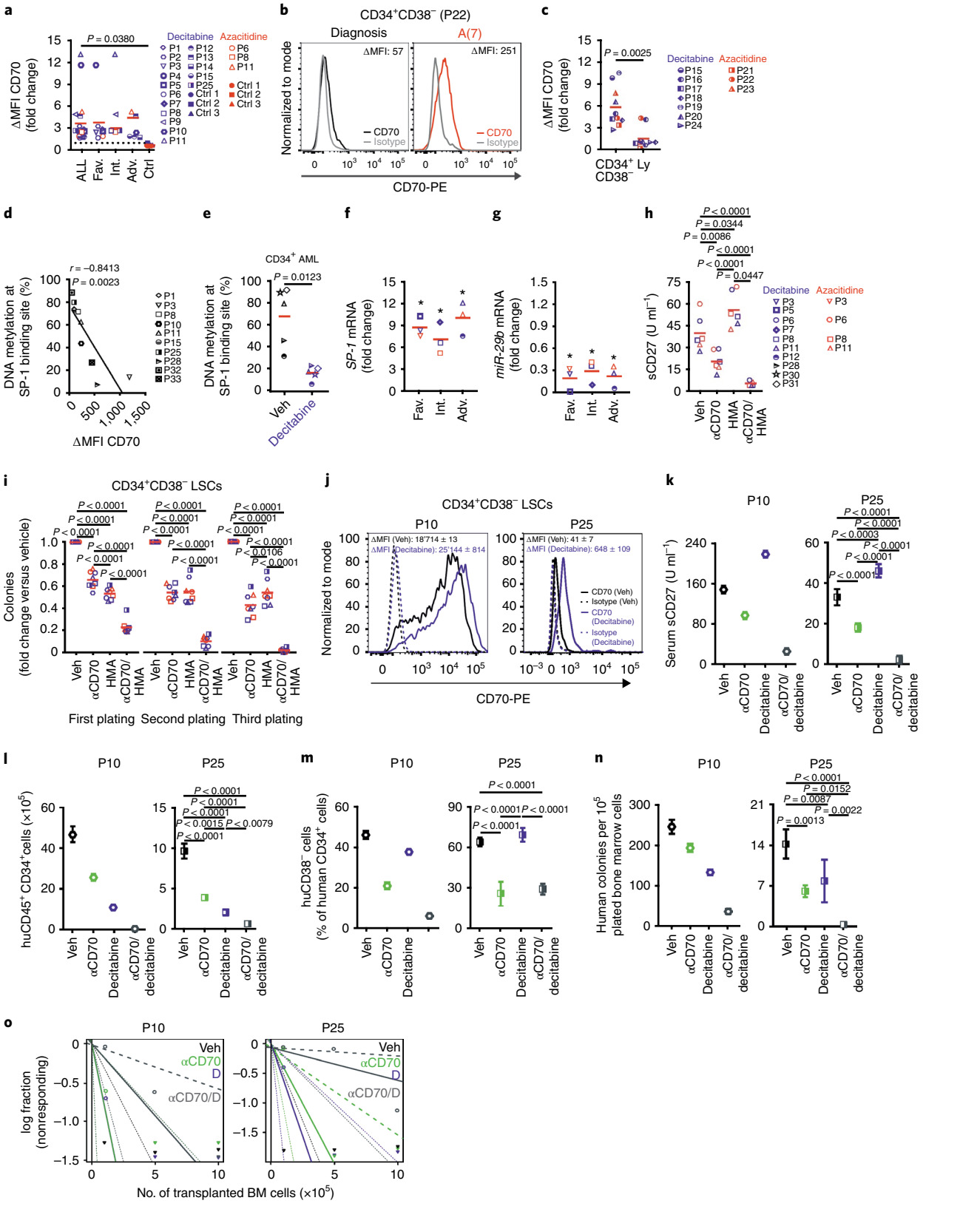

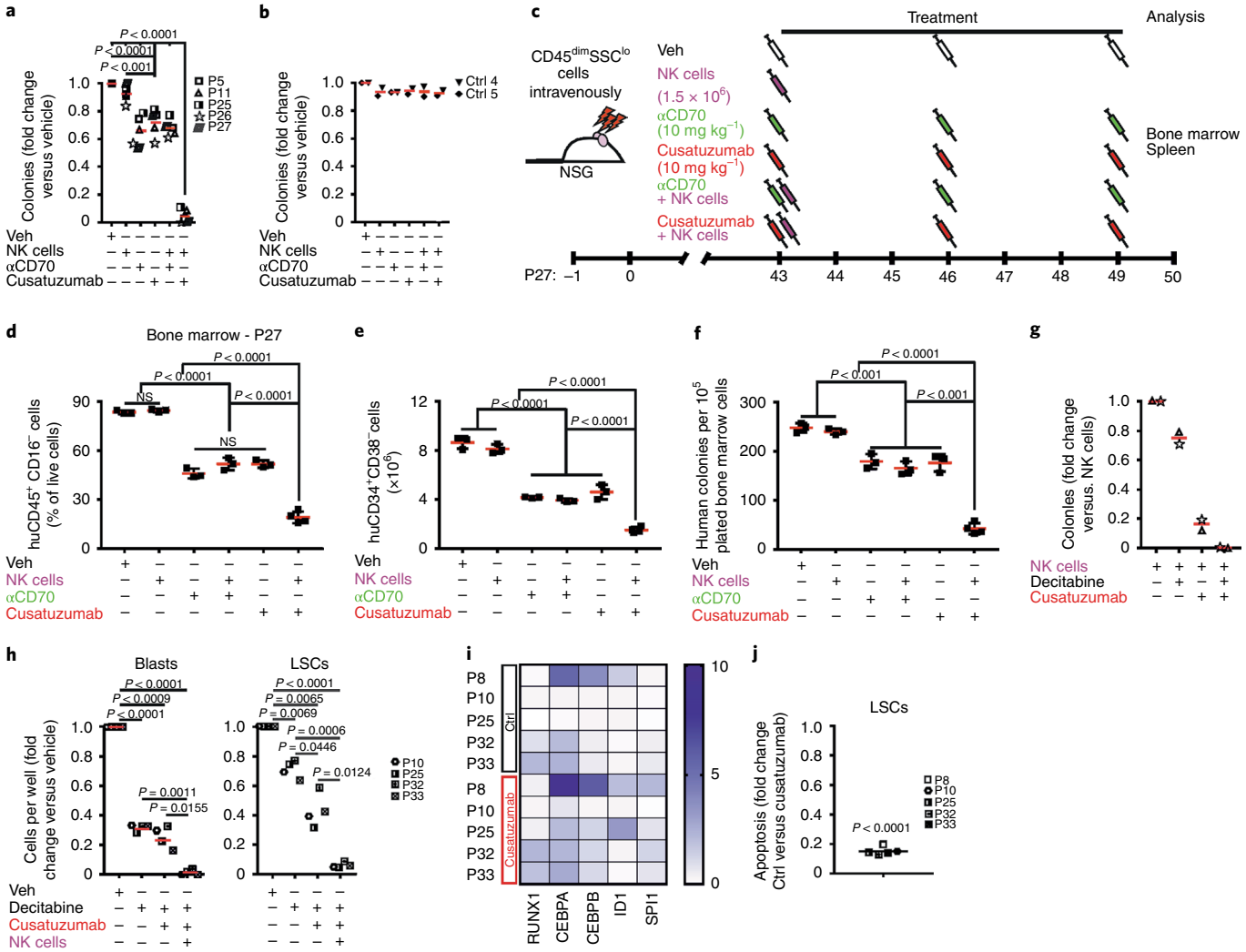

Fig. 2 | The ADCC-enhanced αCD70 mAb cusatuzumab has superior efficacy in reducing LSCs than αCD70 blockade alone. a,**b**, Lin$^-$CD90$^-$CD34$^+$CD38$^-$ LSCs ($n = 5$ patients with AML; P5, P11 and P25–P27) (**a**) and Lin$^-$CD90$^+$CD34$^+$CD38$^-$ HSCs from normal control bone marrow ($n = 2$ controls; Ctrl 4, Ctrl 5) (**b**) were cultured in the presence of different αCD70 mAbs (αCD70 and cusatuzumab) alone or in combination with NK cells (derived from the buffy coats of healthy donors) at a ratio of 1:1 in technical triplicates overnight followed by plating onto methylcellulose. Colony formation was assessed after 14 d. Fold change in colony formation is indicated versus vehicle. Significance was determined using a one-way ANOVA followed by Tukey's multiple comparison tests. **c**–**f**, 5×10^6 FACS-purified CD45^{dim}SSC^{lo} cells from the bone marrow of patient P27 (Supplementary Table 1 and Supplementary Fig. 3) were injected intravenously into sublethally irradiated (2.75 Gy) NSG mice. After engraftment (day 43 after transplantation), mice were randomized to treatment with control mAb, 10 mg kg^{-1} αCD70 mAb or cusatuzumab intraperitoneally (total of 3 injections) alone or in combination with 1.5×10^6 MACS-purified allogenic NK cells derived from the buffy coats of heathy donors (1 injection on day 43; groups: vehicle, NK cells, αCD70, αCD70/NK cells and cusatuzumab: $n = 3$ mice per group; cusatuzumab/NK cells: $n = 4$ mice). One day after the last treatment, animals were killed and the spleen and bone marrow were analyzed. **d**, Frequency of human AML cells (CD45$^+$CD33$^+$) in the bone marrow. Significance was determined using a one-way ANOVA followed by Tukey's multiple comparison test. **e**, Absolute numbers of huCD45$^+$CD34$^+$CD38$^-$ LSCs in the bone marrow. Significance was determined using a one-way ANOVA followed by Tukey's multiple comparison test. **f**, Colony formation of human AML cells; 10^5 bone marrow cells from xenografted AML mice were plated in technical duplicates and AML colonies were enumerated 14 d later. Significance was determined using a one-way ANOVA followed by Tukey's multiple comparison test. **g**, Lin$^-$CD90$^-$CD34$^+$CD38$^-$ LSCs ($n = 2$ patients with AML; P11 and P26) were cultured in the presence of NK cells at a ratio of 1:1 and cusatuzumab alone or in combination with decitabine in technical triplicates overnight followed by plating onto methylcellulose. Colony formation was assessed after 14 d. Fold change in colony formation is indicated versus NK cells. **h**, Lin$^-$CD90$^-$CD34$^+$CD38$^+$ blasts and Lin$^-$CD90$^-$CD34$^+$CD38$^-$ LSCs ($n = 4$ patients with AML; P10, P25, P32 and P33) were cultured with 0.5 μM of decitabine alone or in combination with cusatuzumab (10 μg ml^{-1}) in the presence and absence of NK cells at a ratio of 1:1 in technical triplicates. Cell numbers were assessed after 3 d. The fold change in cell numbers per well is indicated versus vehicle-treated cells. Significance was determined using a one-way ANOVA followed by Tukey's multiple comparison test. **i**,**j**, Lin$^-$CD90$^-$CD34$^+$CD38$^-$ LSCs ($n = 5$ patients with AML; P8, P10, P25, P32 and P33) were cultured in the presence and absence of cusatuzumab (10 μg ml^{-1}) and NK cells (ratio 1:1) in triplicates. The mRNA expression of genes related to differentiation was analyzed by RT-qPCR after 48 h and by annexin V FACS staining after 72 h, respectively. **i**, Heatmap of differentiation-related genes. **j**, Fold change in apoptosis in LSCs ($n = 5$ patients with AML; P8, P10, P25, P32 and P33). Significance was determined using a two-sided one-sample *t*-test (hypothetical value = 1). Data are shown as mean ± s.d. Only statistically significant differences are shown.

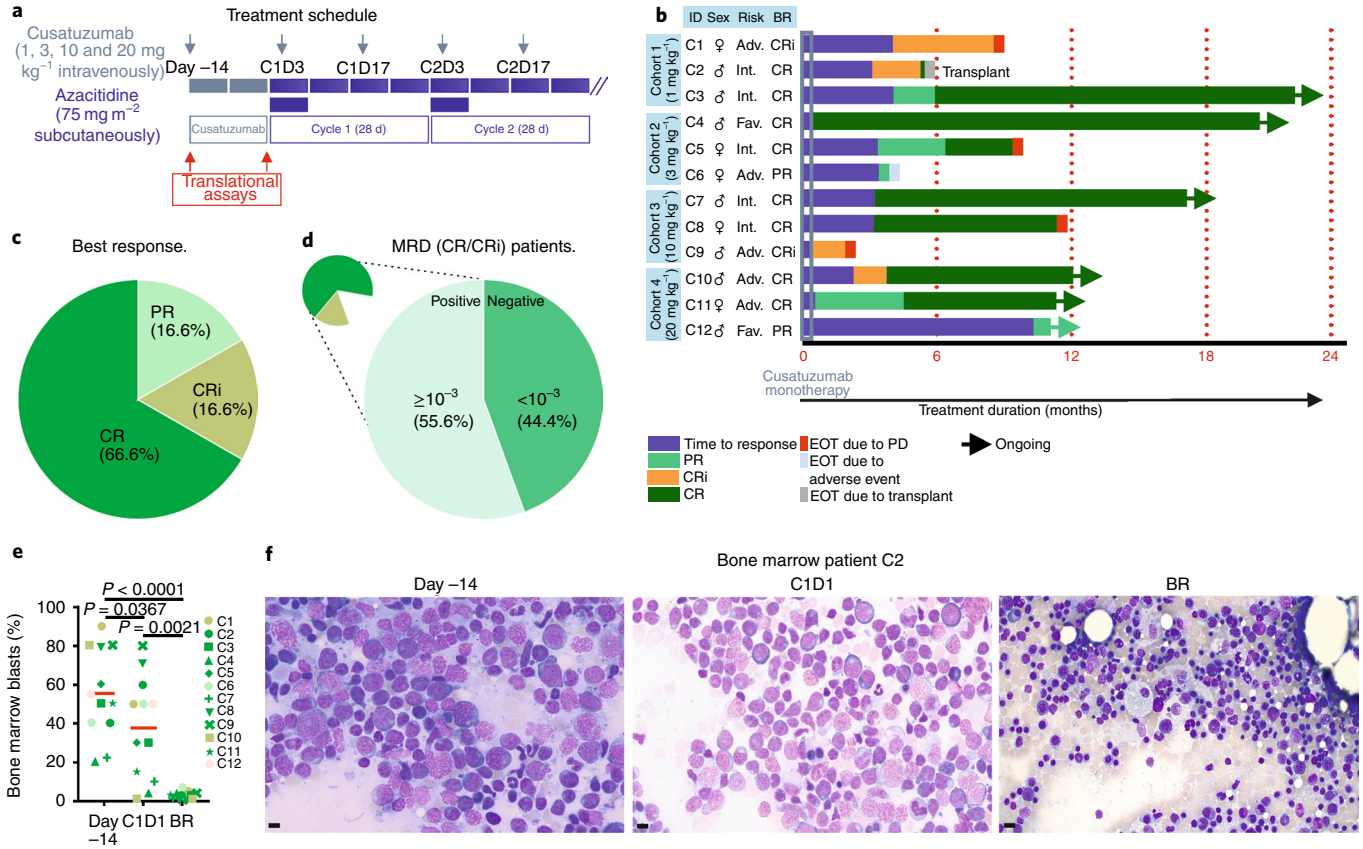

Fig. 3 | Treatment schedule and response. a, Treatment schedule for untreated patients with AML treated with different concentrations of cusatuzumab and azacitidine; 1, 3, 10 and 20 mg kg^{-1} cusatuzumab was given intravenously every second week. Azacitidine was administered subcutaneously at a dose of 75 mg m^{-2} for 7 consecutive days every 4 weeks. **b**, Swimmer plot illustrating the response and outcome of patients with AML treated with cusatuzumab in combination with azacitidine. Adv., adverse risk; Fav., favorable risk; Int., intermediate risk. **c**, Pie chart summarizing the treatment responses. **d**, Pie chart summarizing the MRD assessments in the bone marrow of CR/CRi patients. MRD status is shown for only 9 out of 10 patients in CR/CRi. The bone marrow of patient C9 could not be assessed for MRD status due to a short follow-up (Supplementary Table 8). **e**, Frequency of bone marrow blasts as determined by cytomorphology at day −14, C1D1 and BR ($n = 12$ patients). The bone marrow blasts for patient C12 at time point of best response (BR) are not shown because assessment was not possible due to hypocellular bone marrow. Significance was determined using a two-sided paired *t*-test. **f**, Representative cytomorphology for patient C2 at day −14, C1D1 and BR. The cytomorphology of all samples was assessed once. Scale bar, 10 µm. Data are presented as the mean ± s.d. Only statistically significant differences are shown.

αCD70 and decitabine monotherapy significantly reduced leukemic engraftment in the bone marrow, spleen and blood compared to vehicle-treated AML mice (Supplementary Fig. 2e,f, data not shown). Importantly, cotreatment synergistically reduced the engraftment of $CD45^+Lin^-CD34^-$ and $CD45^+Lin^-CD34^+$ AML cells and $CD45^+Lin^-CD34^+CD38^-$ LSCs in the bone marrow (Fig. 1l,m and Supplementary Fig. 2g,h). Similarly, the more primitive CD45RA-expressing LSCs[20] were reduced after combination treatment (Supplementary Fig. 2i). Decitabine monotherapy had no effect on LSC numbers (Fig. 1m and Supplementary Fig. 2h). Bone marrow cells from αCD70/decitabine-treated mice formed significantly fewer colonies in methylcellulose compared to either monotherapy or untreated controls (Fig. 1n), indicating that AML LSPCs were reduced by αCD70/decitabine treatment. Extreme limiting dilution analysis (ELDA)[21] from the bone marrow of primary PDX AML mice to NSG mice revealed that αCD70/decitabine cotreatment significantly reduced human AML LSCs in PDX mice compared to either monotherapy, as indicated by a substantial reduction in LSC frequency by a factor of 2.9 and 11 in patients P10 and P25, respectively (Fig. 1o and Supplementary Table 2). The PDX results indicate that HMA treatment increased CD70 expression and promoted consecutive CD70/CD27 signaling. The combination with blocking αCD70 mAb synergistically reduced LSC numbers in vivo.

Next, we analyzed whether targeting CD70 with the antibody-dependent cellular cytotoxicity activity (ADCC)-enhanced αCD70 mAb cusatuzumab reduces LSPCs more efficiently than the blocking αCD70 mAb. In the absence of NK cells, cusatuzumab demonstrated a similar capacity in reducing colony formation in vitro as the blocking αCD70 mAb. In the presence of NK cells, cusatuzumab but not 41D12-D mAb treatment further reduced colony formation (Fig. 2a). In contrast, cusatuzumab did not affect colony formation of HSCs from normal control bone marrow (Fig. 2b). To validate our findings in vivo, PDX AML mice were treated either with control mAb, αCD70 mAb or cusatuzumab (Fig. 2c). Cusatuzumab was similarly effective in reducing leukemia cell engraftment and LSC numbers as the blocking αCD70 mAb in the absence of NK cells. However, in the presence of NK cells, cusatuzumab further reduced leukemia engraftment and LSC numbers in the bone marrow and spleen (Fig. 2d,e and Supplementary Fig. 3a–c). The reduction in LSPC numbers in the bone marrow was functionally confirmed by colony-forming assays ex vivo (Fig. 2f).

CD70 upregulation by HMA may render LSCs even more susceptible to direct cytolytic interventions. To test this hypothesis, we performed a drug combination study according to the Chou–Talalay method[22]. Decitabine increased CD70 expression and, in combination with cusatuzumab in the presence of NK cells,

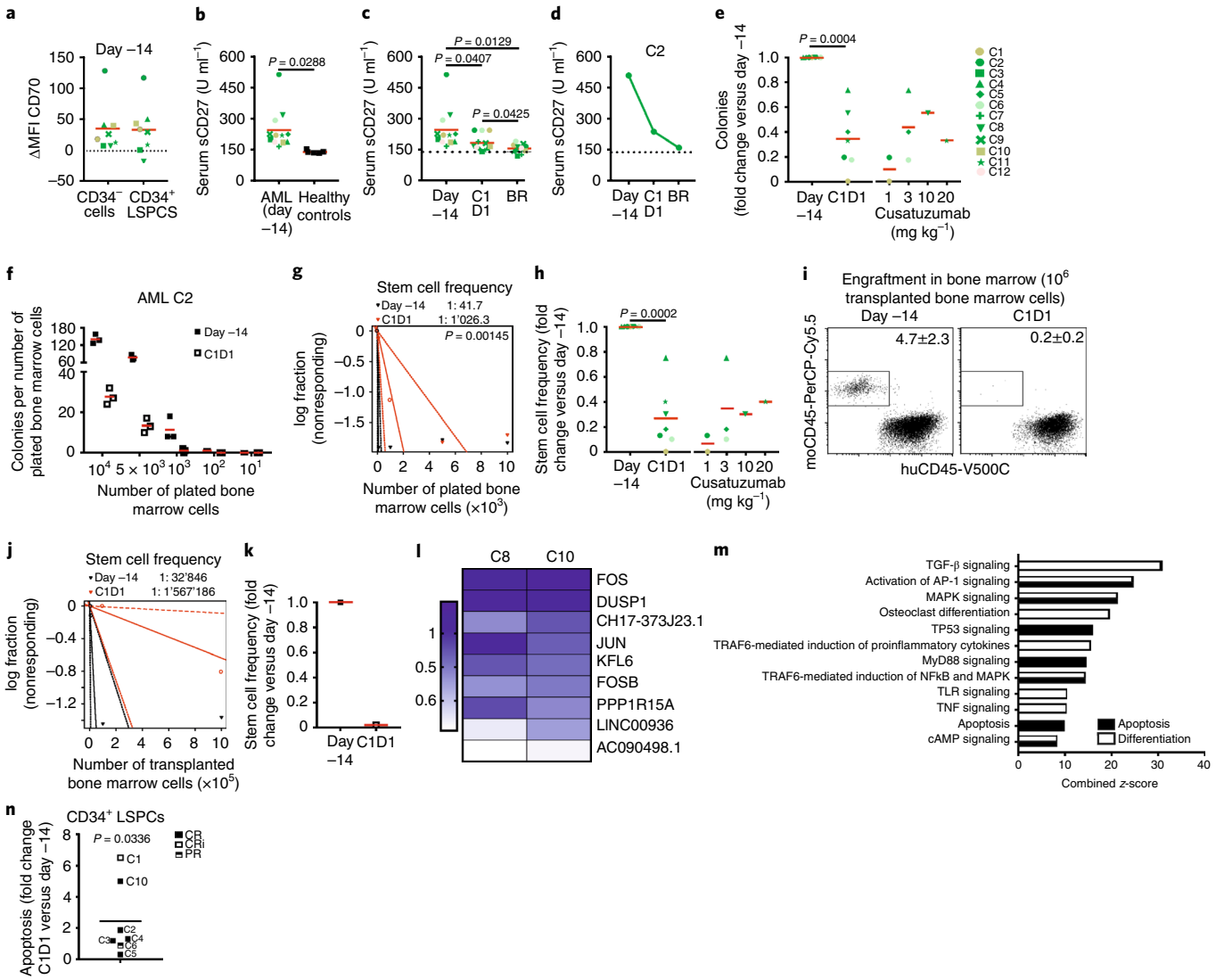

Fig. 4 | Cusatuzumab reduces LSCs in patients with AML. a, CD70 expression on CD34⁻ AML cells and CD34⁺ AML LSPCs in the bone marrow of patients from the study cohort and ($n = 8$ patients) at day −14 (diagnosis). Sufficient material from 8 out of 12 patients enrolled in the study was available to run the analysis. **b**, Serum sCD27 levels from patients with AML on day −14 ($n = 12$ patients) and in the sera of aged-matched healthy donors ($n = 5$). Detection limit of the assay: 0.2 U ml^{-1}. The measurement was performed in technical duplicates. Significance was determined using a two-sided *t*-test. **c**, Serum sCD27 levels at day −14, C1D1 and BR ($n = 12$ patients per time point). The dotted line indicates the mean sCD27 levels of healthy aged-matched controls. The measurement was performed in duplicates. Significance was determined using a repeated measures one-way ANOVA followed by a Tukey's multiple comparisons test. **d**, Serum sCD27 levels from patient C2 of the study cohort at day −14, C1D1 and BR, measured in technical duplicates. **e**, Fold change in colony formation for selected patients of the study cohort ($n = 7$). Sufficient material from 7 out of 12 patients enrolled in the study was available to run the analysis. Colony assays were performed in technical triplicates. Significance was determined using a two-sided paired *t*-test. **f**, Colony formation at a limiting dilution for patient C2 at day −14 and C1D1 performed in technical triplicates. **g**, LSC frequencies for patient C2 estimated using ELDA. Colony assays were performed in technical triplicates ($n = 1$ patient C2). LSC frequencies were estimated with the ELDA software. **h**, LSC frequencies for all patients with sufficient cells in bone marrow aspirates performed in technical triplicates ($n = 7$ patients with AML). Only sufficient material from 7 out of 12 patients enrolled in the study was available to run the analysis. Significance was determined using a two-sided paired *t*-test. **i**–**k**, T cell-depleted FACS-purified bone marrow cells from patient C2 at day −14 and C1D1 were injected at titrated numbers (10^6, $2{,}5 \times 10^5$, 10^5 and 10^4) into sublethally irradiated (2.75 Gy) NSG mice ($n = 2$ mice per cell number injected). Engraftment was assessed after 16 weeks in the bone marrow by FACS. The detection limit for positive engraftment was set as 0.1% human bone marrow cells (CD45⁺CD33⁺). **i**, Representative FACS plots of the engraftment of human cells in the bone marrow of PDX mice from patient C2. Data from one single experiment are shown. **j**, LSC frequencies estimated using ELDA. A frequency >0.1% of human cells (huCD45⁺CD33⁺) in the murine bone marrow was rated as positive engraftment[1,28]. LSC frequencies were estimated with the ELDA software. **k**, Fold change in stem cell frequency. **l**, Heatmap. Common differentially regulated genes after cusatuzumab treatment in the LSPCs of patients C8 and C10 identified via scRNA-seq. **m**, Histogram of GO enrichment analysis of the biological pathways significantly affected in Lin⁻CD34⁺ AML cells after cusatuzumab monotherapy. **n**, Fold change in apoptosis in Lin⁻CD90⁻CD34⁺ LSPCs in the bone marrow of patients with AML at C1D1 versus day −14 as analyzed by annexin V FACS staining ($n = 7$ patients). Significance was determined using a two-sided one-sample *t*-test (hypothetical value = 1). Data are presented as the mean. Only statistically significant differences are shown.

synergistically killed CD70-expressing MOLM-13 cells and NOMO-1 cells in a broad dose range (Supplementary Fig. 4a–i).

Next, we treated human LSCs and blasts with cusatuzumab or decitabine monotherapy or in combination and assessed colony formation. Although AML blasts do not upregulate CD70 on treatment with HMA (Supplementary Fig. 1e), CD70 is expressed on both LSCs and blasts[11]. Indeed, cusatuzumab/HMA cotreatment in the presence of NK cells effectively eliminated both LSCs and blasts compared to all other treatment groups (Fig. 2g,h). Decitabine monotherapy quite efficiently eliminated blasts but only marginally reduced LSCs. Only the combination with cusatuzumab eliminated LSCs. Cusatuzumab treatment uniformly promoted the expression of myeloid differentiation genes such as *SPI1* (*PU.1*) and *CEBPA* and reduced cell viability on average by approximately 85% compared to control treatment (Fig. 2i,j).

These results indicate that a combination of HMA with the ADCC-enhanced αCD70 mAb cusatuzumab eliminates LSCs synergistically and more efficiently than in combination with an αCD70-blocking mAb.

Based on our preclinical data, we designed a phase 1/2 trial to study the safety, tolerability and efficacy of cusatuzumab as monotherapy and in combination with azacitidine (EudraCT no. 2016-002151-17; see Methods). Untreated patients with AML, including de novo, secondary and therapy-related AML, not fit for intensive chemotherapy were included in the study. Azacitidine was administered at a standard dose of 75 mg m^{-2} subcutaneously for 7 consecutive days every 28 d. Cusatuzumab was infused on day 3 when CD70 was upregulated on LSCs by HMA and on day 17 of each treatment cycle. A first infusion of cusatuzumab at day −14, in the absence of azacitidine, enabled us to study the effect of cusatuzumab monotherapy (Fig. 3a).

The clinical data cutoff for phase 1 was 18 February 2019, with the primary objective to determine the maximum tolerated dose (MTD) of cusatuzumab and the recommended dose for phase 2 in combination with azacitidine. Twelve untreated patients with AML with a median age of 75 years (range, 64–84) were enrolled in four sequential dose cohorts of cusatuzumab (1, 3, 10 or 20 mg kg^{-1}; 3 patients per dose cohort) in the dose escalation part of the trial (Fig. 3a and Supplementary Table 3). Patients had adverse ($n=5$), intermediate ($n=5$) and favorable ($n=2$) European LeukemiaNet (ELN) risk features based on genotype and cytogenetics[15]. No dose-limiting toxicities were reported and the MTD of cusatuzumab was not reached.

All 12 patients had at least 1 treatment emergent adverse event (TEAE; total of 167 events) and all 12 patients had at least one grade ≥3 TEAE (71 events). Nine patients had drug-related TEAEs (17 events); of these, two patients experienced infusion-related reactions (6 events). Treatment emergent serious adverse events were reported for 9 patients (19 events); two of these were drug-related serious adverse events reported for a single patient (Supplementary Tables 4–6).

Hematological toxicities related to azacitidine were the most frequent TEAE (34 events in 10 patients)[3]. The only patient with early death succumbed to the progression of AML. In addition, no increase of viral or fungal infections was observed.

Cusatuzumab monotherapy did not affect the numbers of $CD4^+$ and $CD8^+$ T cells in peripheral blood, two cell populations known to transiently express CD70 during immune activation[7]. In contrast, the $CD4^+/CD8^+$ T cell ratio slightly increased after cusatuzumab monotherapy (Supplementary Fig. 5). Long-term exposure of patients to the cusatuzumab/azacitidine combination treatment did not affect normal hematopoiesis as indicated by normal blood counts and leukocyte differential in the 6 patients treated for longer than 6 months at the time point of data cutoff on 18 February 2019 (Supplementary Table 7).

In phase 1 of the clinical trial, the best hematological response was complete remission (CR) in 8 patients, incomplete blood count recovery (CRi) in 2 patients and PR in 2 patients (Fig. 3b,c and Supplementary Table 8). Thus, 10 out of 12 patients achieved a CR/CRi. Responses were observed at all dose levels of cusatuzumab and the median time to response was 3.3 months. Importantly, responses were durable with 6 patients, who were still on study treatment at the time of data cutoff and median progression-free survival had not been reached yet. Four out of 9 evaluable patients (44%) with CR/CRi achieved minimal residual disease (MRD) negativity by flow cytometry in the bone marrow at a threshold of 10^{-3} (Fig. 3d and Supplementary Table 8). End of treatment (EOT) was caused by progression in four patients, by referral to allogeneic transplantation in CR in patient C2 and by treatment-related toxicity (hypertension) in one patient.

Importantly, cusatuzumab monotherapy reduced bone marrow blasts in only 2 weeks in all patients, on average to 32%, with three responders (1 CR, 1 CRi and 1 PR) among the 12 patients. The combination with azacitidine further reduced the bone marrow blast counts by 92% compared to C1D1 (Fig. 3e,f). No correlation between response to cusatuzumab treatment and the numbers and frequencies of NK cells in peripheral blood at day −14 could be observed (Supplementary Fig. 6).

CD70 expression was detectable on $CD34^-$ AML cells and LSPCs in most patients (Fig. 4a). To monitor the degree of CD70/CD27 interaction in the patients in vivo, we assessed sCD27 levels in the sera of patients enrolled in the study at day −14. sCD27 levels were significantly increased in all patients with AML compared to healthy age-matched controls (Fig. 4b). Cusatuzumab monotherapy significantly reduced sCD27 levels within 14 d of treatment (Fig. 4c). The combination of azacitidine with cusatuzumab further decreased sCD27 at the time point of best response (BR) to levels comparable to healthy age-matched controls (Fig. 4c,d).

Cusatuzumab monotherapy reduced LSPC numbers by a factor of 3, as assessed by the colony-forming capacity of plated total bone marrow cells (Fig. 4e). ELDA revealed that monotherapy with cusatuzumab significantly reduced LSC numbers compared to day −14 in all patients analyzed (Fig. 4f–h).

The in vitro experiments did not allow to unambiguously distinguish between LSPCs and normal hematopoietic stem/progenitor cells. The most stringent experiment to assess LSC numbers is to analyze engraftment of titrated numbers of bone marrow cells after transplantation into sublethally irradiated NSG mice (Fig. 4i). ELDA indicated that cusatuzumab monotherapy in patient C2 reduced the LSC frequency by approximately 47-fold (Fig. 4j,k). These data suggest that targeting CD70 by cusatuzumab monotherapy reduces LSCs in patients with AML.

To address the molecular mechanism of cusatuzumab on AML LSCs, we performed single-cell RNA sequencing (scRNA-seq) of FACS-purified Lin^-CD34^+ AML cells from patients C8 and C10 at day −14 and after cusatuzumab monotherapy (C1D1) (Supplementary Fig. 7a–c). Patient C10 harbored two AML clones that differed in the expression of CD34; the $CD34^+$ clone was purified and included in the scRNA-seq analysis (Supplementary Table 3). To focus on malignant cells, we took advantage of the molecular mutations identified at diagnosis in patients C8 (*DNMT3a*) and C10 (*ASXL1*, *EZH2*, *RUNX1*, *SH2B3*, *ZRSR2*) using a data crushing approach separating cells that did or did not express the molecular marker. This approach identified a frequency of 77 and 74% of malignant AML cells at day −14 and C1D1 for patient C8, respectively, and 99.9% for patient C10 at both time points. No distinct clusters could be identified in principal component analysis of the single cells of patients C8 and C10 at diagnosis or after cusatuzumab monotherapy, suggesting the predominance of a clonal population with similar cellular states (Supplementary Fig. 7d). We identified 47 and 18 differentially expressed genes after cusatuzumab monotherapy for patients C8 and C10, respectively (Supplementary Fig. 7e–h and Supplementary Tables 9 and 10). Patients C8

and C10 shared 9 differentially expressed genes (7 mRNAs and 2 lncRNAs; Fig. 4l). GO analysis of these 9 genes revealed a preferential involvement in TGF-β, AP-1, MAPK, cAMP, TNF and MyD88 signaling and induction of proinflammatory cytokines all associated with myeloid cell differentiation and/or apoptosis (Fig. 4m).

Lastly, we assessed the level of apoptotic Lin$^-$CD34$^+$ LSPCs at day −14 and C1D1 in 7 out of 12 patients by annexin V staining. After cusatuzumab treatment (C1D1), the frequency of apoptotic cells was significantly increased compared to day −14 (Fig. 4n). Collectively, these data suggest that cusatuzumab treatment triggers differentiation and apoptosis in LSPCs.

The CD70/CD27 interaction maintains the self-renewal of AML LSCs by activating Wnt signaling and by promoting symmetrical cell division[11]. Since CD70 is only transiently expressed on activated lymphocytes but not during homeostasis[7], targeting the CD70/CD27 interaction may allow selective elimination of CD70-expressing LSCs. In the present study, we document CD70 upregulation and reinforced CD70/CD27 signaling on LSCs in response to HMA treatment. Increased expression of CD70 offers two therapeutic strategies to selectively target LSCs. First, blocking the CD70/CD27 interaction reduces CD27/TNIK/Wnt signaling and self-renewal of LSCs and induces differentiation[11]. Second, the unique expression pattern of CD70 allows for direct cytolytic targeting[11,23]. We explored both possibilities in vitro and in a limited number of xenotransplantation experiments using an αCD70 mAb with deficiency in effector function due to E233P/L234V/L235A amino acid substitutions in the CH2 region[18,19] and an ADCC-enhanced version of the same clone (cusatuzumab)[19,24]. Both blocking CD70/CD27 signaling and ADCC-mediated target cell killing synergistically eliminated LSCs. However, cusatuzumab was clearly superior to the blocking-only variant of the antibody. Therefore, cusatuzumab was tested in a phase 1/2 trial together with azacitidine. Within only two weeks, cusatuzumab monotherapy reduced blast counts in the bone marrow on average to 32% with two patients reaching CR (1 CR, 1 CRi) and one patient reaching PR. In addition, cusatuzumab monotherapy significantly reduced LSCs up to 50-fold.

The overall response rate for the combination of cusatuzumab with azacitidine was 100% (8 CR, 2 CRi, 2 PR) with 44% of patients with CR/CRi achieving flow MRD negativity in the bone marrow. Responses were observed in all dose levels of cusatuzumab. Although this phase 1 study only included 12 patients, the observed response rate favorably compares with historical data on HMA monotherapy[3,4].

Different compounds have been tested in combination with low-dose cytarabine or HMAs in older unfit patients with AML (reviewed in Perl[25]). Similar to cusatuzumab, venetoclax eliminates LSCs, albeit by a different mechanism, that is, by suppressing oxidative phosphorylation[26].

In conclusion, cusatuzumab monotherapy and in combination with azacitidine is highly active in previously untreated patients with AML unfit for intensive chemotherapy. Cusatuzumab eliminates CD70-expressing LSCs potentially leading to deep and durable remissions. Ongoing and future clinical phase 2 and 3 studies will further investigate the potential of cusatuzumab to induce durable responses and deep remissions in combination with HMA in more patients.

Online content

Any methods, additional references, Nature Research reporting summaries, source data, extended data, supplementary information, acknowledgements, peer review information; details of author contributions and competing interests; and statements of data and code availability are available at https://doi.org/10.1038/s41591-020-0910-8.

Received: 10 April 2019; Accepted: 27 April 2020;
Published online: 29 June 2020

References

1. Lapidot, T. et al. A cell initiating human acute myeloid leukaemia after transplantation into SCID mice. *Nature* **367**, 645–648 (1994).
2. Thomas, D. & Majeti, R. Biology and relevance of human acute myeloid leukemia stem cells. *Blood* **129**, 1577–1585 (2017).
3. Dombret, H. et al. International phase 3 study of azacitidine vs conventional care regimens in older patients with newly diagnosed AML with >30% blasts. *Blood* **126**, 291–299 (2015).
4. Kantarjian, H. M. et al. Multicenter, randomized, open-label, phase III trial of decitabine versus patient choice, with physician advice, of either supportive care or low-dose cytarabine for the treatment of older patients with newly diagnosed acute myeloid leukemia. *J. Clin. Oncol.* **30**, 2670–2677 (2012).
5. Craddock, C. et al. Azacitidine fails to eradicate leukemic stem/progenitor cell populations in patients with acute myeloid leukemia and myelodysplasia. *Leukemia* **27**, 1028–1036 (2013).
6. Bowman, M. R. et al. The cloning of CD70 and its identification as the ligand for CD27. *J. Immunol.* **152**, 1756–1761 (1994).
7. Nolte, M. A., van Olffen, R. W., van Gisbergen, K. P. J. M. & van Lier, R. A. W. Timing and tuning of CD27–CD70 interactions: the impact of signal strength in setting the balance between adaptive responses and immunopathology. *Immunol. Rev.* **229**, 216–231 (2009).
8. Liu, N., Sheng, X., Liu, Y., Zhang, X. & Yu, J. Increased CD70 expression is associated with clinical resistance to cisplatin-based chemotherapy and poor survival in advanced ovarian carcinomas. *Onco Targets Ther.* **6**, 615–619 (2013).
9. Ge, H. et al. Tumor associated CD70 expression is involved in promoting tumor migration and macrophage infiltration in GBM. *Int. J. Cancer* **141**, 1434–1444 (2017).
10. Bertrand, P. et al. The costimulatory molecule CD70 is regulated by distinct molecular mechanisms and is associated with overall survival in diffuse large B-cell lymphoma. *Genes Chromosome. Canc.* **52**, 764–774 (2013).
11. Riether, C. et al. CD70/CD27 signaling promotes blast stemness and is a viable therapeutic target in acute myeloid leukemia. *J. Exp. Med.* **214**, 359–380 (2017).
12. Lu, Q., Wu, A. & Richardson, B. C. Demethylation of the same promoter sequence increases CD70 expression in lupus T cells and T cells treated with lupus-inducing drugs. *J. Immunol.* **174**, 6212–6219 (2005).
13. Cashen, A. F., Schiller, G. J., O'Donnell, M. R. & DiPersio, J. F. Multicenter, phase II study of decitabine for the first-line treatment of older patients with acute myeloid leukemia. *J. Clin. Oncol.* **28**, 556–561 (2010).
14. Marcucci, G., Silverman, L., Eller, M., Lintz, L. & Beach, C. L. Bioavailability of azacitidine subcutaneous versus intravenous in patients with the myelodysplastic syndromes. *J. Clin. Pharmacol.* **45**, 597–602 (2005).
15. Döhner, H. et al. Diagnosis and management of AML in adults: 2017 ELN recommendations from an international expert panel. *Blood* **129**, 424–447 (2017).
16. Liu, S. et al. Sp1/NFκB/HDAC/*miR-29b* regulatory network in KIT-driven myeloid leukemia. *Cancer Cell* **17**, 333–347 (2010).
17. Garzon, R. et al. MicroRNA-29b induces global DNA hypomethylation and tumor suppressor gene reexpression in acute myeloid leukemia by targeting directly *DNMT3A* and *3B* and indirectly *DNMT1*. *Blood* **113**, 6411–6418 (2009).
18. Armour, K. L., Clark, M. R., Hadley, A. G. & Williamson, L. M. Recombinant human IgG molecules lacking Fcγ receptor I binding and monocyte triggering activities. *Eur. J. Immunol.* **29**, 2613–2624 (1999).
19. Silence, K. et al. ARGX-110, a highly potent antibody targeting CD70, eliminates tumors via both enhanced ADCC and immune checkpoint blockade. *MAbs* **6**, 523–532 (2014).
20. Kersten, B. et al. CD45RA, a specific marker for leukaemia stem cell sub-populations in acute myeloid leukaemia. *Br. J. Haematol.* **173**, 219–235 (2016).
21. Hu, Y. & Smyth, G. K. ELDA: extreme limiting dilution analysis for comparing depleted and enriched populations in stem cell and other assays. *J. Immunol. Methods* **347**, 70–78 (2009).
22. Chou, T.-C. Drug combination studies and their synergy quantification using the Chou–Talalay method. *Cancer Res.* **70**, 440–446 (2010).
23. Perna, F. et al. Integrating proteomics and transcriptomics for systematic combinatorial chimeric antigen receptor therapy of AML. *Cancer Cell* **32**, 506–519.e5 (2017).
24. Shinkawa, T. et al. The absence of fucose but not the presence of galactose or bisecting *N*-acetylglucosamine of human IgG1 Complex-type oligosaccharides shows the critical role of enhancing antibody-dependent cellular cytotoxicity. *J. Biol. Chem.* **278**, 3466–3473 (2003).

25. Perl, A. E. The role of targeted therapy in the management of patients with AML. *Hematology Am. Soc. Hematol. Educ. Progr.* **2017**, 54–65 (2017).
26. Pollyea, D. A. et al. Venetoclax with azacitidine disrupts energy metabolism and targets leukemia stem cells in patients with acute myeloid leukemia. *Nat. Med.* **24**, 1859–1866 (2018).
27. Veselý, J. & Cihák, A. Incorporation of a potent antileukemic agent, 5-aza-2′-deoxycytidine, into DNA of cells from leukemic mice. *Cancer Res.* **37**, 3684–3689 (1977).
28. Paczulla, A. M. et al. Long-term observation reveals high-frequency engraftment of human acute myeloid leukemia in immunodeficient mice. *Haematologica* **102**, 854–864 (2017).

Methods

Detailed information on experimental design and reagents can be found in the Nature Research Reporting Summary.

Animals. NSG mice were purchased from Charles River Laboratories; 6- to 8-week-old male and female mice were housed under specific pathogen-free conditions in individually ventilated cages with food and water provided ad libitum and were regularly monitored for pathogens. All animals used in the experiments were age- and sex-matched. Randomization of mice into treatment groups was performed using the random number generator in Prism v.7.0 (GraphPad Software). Experiments were conducted and analyzed in a nonblinded fashion. Details on repetitions and replicates are shown in the figure legends. Experiments were approved by the local experimental animal committee of the Canton of Bern and performed according to Swiss laws for animal protection (BE75/17 and BE78/17).

Cell lines. MOLM-13 and NOMO-1 cells were purchased from ATCC. The authors performed no additional authentication. Each cell line was tested *Mycoplasma*-free and grown in FCS-containing medium, as recommended by ATCC, with GlutaMAX supplemented with 100 U ml^{-1} of penicillin and 100 µg ml^{-1} of streptomycin in a humidified atmosphere of 95% air and 5% CO_2 at 37 °C.

Patients samples for the preclinical experiments. Peripheral blood samples and bone marrow aspirates were obtained from untreated patients with AML at diagnosis and HMA-treated patients with AML at the University Hospital of Bern between 2014 and 2017 (Supplementary Table 1). Written informed consent was collected from all patients involved in the study. Study data were collected and managed using the research electronic data capture tools hosted at the Department for BioMedical Research[29]. Diagnostic bone marrow aspirates that were considered normal according to the hematologist and a surgical pathologist were used as controls.

Serum samples from older healthy donors ($n = 5$; 69.2 ± 1.8 years) and the buffy coats from healthy donors were obtained from the regional blood transfusion service in Bern. Analysis of samples was approved by the Bern local ethical committee (KEK 122/14).

Antibodies, flow cytometry and reagents for treatment. The following antibodies were used (all BioLegend): αCD34-APC (1:80; catalog no. 343607, clone 561); αCD34-PE (1:100; catalog no. 343603, clone 561); αCD38-PE-Cy7 (1:50; catalog no. 303515, clone HIT2); αCD90-PerCP-Cy5.5 (1:100; catalog no. 382113, clone 5E10); αCD33-PerCP-Cy5.5 (1:100; catalog no. 302413, clone WM53); CD45RA-APC-Cy7 (1:20; catalog no. 304151, clone HI100); αCD8a-PerCP-Cy5.5 (1:100; catalog no. 300923, clone HIT8a); αCD4-PerCP-Cy5.5 (1:100; catalog no. 344607, clone SK3); CD19-APC-Cy7 (1:100; catalog no. 302217, clone HIB19); mouse-αCD45-PerCP-Cy5.5 (1:200; catalog no. 103131, clone 30-F11); mouse-αCD45-PE-Cy7 (1:200; catalog no. 103113, clone 30-F11); and annexin-V-Pacific blue (1:50). Lineage-positive cells were excluded by staining using biotinylated αCD2 (1:100; catalog no. 300203, clone RPA-2.10); αCD3 (1:100; catalog no. 317319, clone OKT3); aCD14 (1:100; catalog no. 325623, clone HCD14); αCD16 (1:100; catalog no. 302003, clone 3G8); αCD19 (1:100; catalog no. 302203, clone HIB19); αCD56 (1:100; catalog no. 318319, clone HCD56); and αCD235 (1:100; catalog no. 306617, clone HIR2), followed by a second step using streptavidin-FITC conjugate (1:3,000; BD Biosciences). αCD70-PE (1:10; catalog no. 555835, clone KI-24) and corresponding isotype control mAb were obtained from BD Biosciences. The viability dye eFluor 450 was sourced from eBiosciences (1:1,000). αCD45-V-500C (1:50; catalog no. 56077, clone 2DI) was obtained from BD Biosciences.

Flow cytometry analysis on whole bone marrow was performed after red blood cell lysis. Samples were analyzed on a BD LSRFortessa (BD Biosciences) and sorting was performed using a BD FACSAria III (BD Biosciences). Data were collected using the FACSDiva software v8.0.1 (BD Biosciences) and analyzed using the FlowJo software 10.6.2 (FlowJo LLC). Effective separation after FACS sorting was assessed by reanalyzing a fraction of the sorted samples by flow cytometry analysis (purity after FACS sorting: 95.3 ± 1.3%). The human αCD70 mAb specifically blocks the CD70/CD27 interaction with deficiency in effector functions by E233P/L234V/L235A amino acid substitutions in the CH2 domain of the parental clone 41D12-D (refs. [18,19]); cusatuzumab and pavilizumab (mock treatment) were obtained from argenx.

RNA isolation and reverse transcription–quantitative PCR (RT–qPCR). For RT–qPCR, total RNA was extracted using the RNeasy Mini Kit (QIAGEN). cDNA synthesis was performed using the High-Capacity cDNA Reverse Transcription Kit (Applied Biosystems). Gene expression analysis was performed using self-designed primers for *CD70* (forward 5′-TGCTTTGGTCCCATTGGTC-3′; reverse 5′-TACGTCCCACCCAAGTGAC)-3′, *CEBPA* (forward 5′-AGACCTAGAGATCTGGCTGTG-3′; reverse 5′-GGACTGATCGTGCTTCGTG-3′), *CEBPB* (forward 5′-TTTCGAAGTTGATGCAATCGG-3′; reverse 5′-AAACATCAACAGCAACAAGCC-3′), *ID1* (forward 5′-TGTTACTCACGCCTCAAGGA-3′; reverse 5′-CTGAAGGTCCCTGATGTAGTC-3′), *RUNX1* (forward 5′-GCTTCACTCTGACCATCACTG-3′; reverse 5′-TGCCGATGTCTTCGAGGT-3′), *SPI1* (forward 5′-CCTCAGCCATCAGAAGACCT-3′; reverse 5′-CAGTAATGGTCGCTATGGCTC-3′), *SP-1* (forward 5′-AGAGGCCATTTATGTGTACCTG-3′; reverse 5′-AGGGCAGGCAAATTTCTTCTC-3′) and *GAPDH* (forward 5′-TCATTTCCTGGTATGACAACGA-3′; reverse 5′-CTTCCTCTTGTGCTCTTGCTG-3′) using the SYBR Green reaction. RT–qPCR reactions were performed in duplicate including nontemplate controls using an ABI Prism 7500 Sequence Detection System (Applied Biosystems). Relative quantification of gene expression was normalized against a reference gene (*GAPDH*) and calculated as $2^{-\Delta c_T}$.

MicroRNA analysis. Total RNA was extracted using the RNeasy Micro Kit (Qiagen) and cDNA was synthesized using the High-Capacity cDNA Reverse Transcription Kit (Applied Biosystems). MicroRNA concentrations were measured using TaqMan microRNA assays for *miR-29b* or *RNU48* (Applied Biosystems); RT–qPCR results were normalized to *RNU48* expression.

Liquid cultures. A total of 1×10^5 FACS-purified CD34$^+$CD38$^-$ LSCs from the bone marrow of patients with AML or HSCs from normal control bone marrow (Supplementary Table 1) were cultured in StemSpan SFEM medium (STEMCELL Technologies) supplemented with human cytokines (StemSpan CC100) in the presence or absence of 10 mg ml^{-1} αCD70 mAb or 0.5 µM of decitabine or azacitidine alone or in combination in 96-well plates at 37 °C and 5% CO_2. The numbers of viable cells were assessed by trypan blue or viability dye staining. CD70 mRNA and protein expression and sCD27 levels were determined after 3 d of culture.

Colony assays. Colony assays of FACS-purified CD34$^+$CD38$^-$ LSCs from the peripheral blood or bone marrow of patients newly diagnosed with AML or normal control bone marrow (Supplementary Table 1) were performed as described previously with slight modifications[30]. Briefly, 1×10^3 CD34$^+$CD38$^-$ cells were cultured overnight in 96-well plates at 37 °C and 5% CO_2 in StemSpan SFEM medium in the presence or absence of 10 mg ml^{-1} αCD70 mAb or 0.5 µM decitabine or azacitidine alone or in combination followed by plating into MethoCult H4435 enriched medium (methylcellulose; STEMCELL Technologies). αCD70 and HMA were added in the first cultures but not during replating. Sterile DMSO and control mAb specific for the F protein of respiratory syncytial virus (palivizumab) were used as the mock treatment. Colonies and cells were enumerated after 14 d (≥30 cells per colony). For serial replating experiments, 10^4 cells were collected from preceding colony assays and were replated in methylcellulose without further addition of mAb or HMA. Colonies were enumerated 14 d later.

Murine PDX AML model and limiting dilution experiments. PDX experiments were performed as described previously[11]. NSG mice were sublethally irradiated (2.75 Gy) on the day before injection. Then, 5×10^6 FACS-purified CD45^{dim}SSC^{lo} from the bone marrow of patients newly diagnosed with AML (patients P10, P25 and P27; Supplementary Table 1) were injected intravenously into the tail vein. The CD34$^+$ cell frequencies were as follows: PDX of P10: 90.4 ± 0.2; PDX of P25: 5.8 ± 0.8; and PDX of P27: 81,8 ± 1.0.

Five (P10), 12 (P25) and 6 (P27) weeks after transplantation, mice were randomized using the random number generator of Prism into the different treatment groups as specified in the respective figure legends.

For the analysis of bone marrow in xenografted AML mice, the immunophenotype of LSCs was defined as Lin$^-$CD34$^+$CD38$^-$ cells according to refs. [1,31,32].

For the limiting dilution assays, whole bone marrow cells from treated primary AML xenograft mice or study patients with AML at diagnosis and after cusatuzumab monotherapy were transplanted at titrated numbers into sublethally irradiated (2.75 Gy) secondary recipients; engraftment in blood, spleen and bone marrow was assessed at the time points shown in the figure legends. A frequency >0.1% of human cells (huCD45$^+$CD33$^+$) in the murine bone marrow was rated as positive engraftment.

To study LSC frequencies for patient C2 at day −14 and C1D1 in vivo, FACS-purified T cell-depleted bone marrow cells were injected at titrated numbers into sublethally irradiated (2.75 Gy) secondary recipients. Engraftment was assessed after 16 weeks in the bone marrow by FACS. A frequency >0.1% of human cells (huCD45$^+$CD33$^+$) in the murine bone marrow was rated as positive engraftment.

sCD27 measurements. sCD27 levels in cell supernatants and in the serum of PDX mice were analyzed by ELISA as described previously in Riether et al.[11]. sCD27 in serum from patients enrolled in the clinical trial was measured in duplicate using the CD27 (Soluble) Human Instant ELISA Kit (Invitrogen). The detection limit of the assay was 0.2 U ml^{-1}.

DNA methylation analysis of the *CD70* promoter. The methylation of the SP-1 binding site at the *CD70* promoter was analyzed in FACS-purified Lin$^-$CD90$^-$CD34$^+$CD38$^-$ AML LSCs and Lin$^-$CD90$^+$CD34$^+$CD38$^-$ HSCs from patients newly diagnosed with AML and healthy donors as well as from Lin$^-$CD90$^-$CD34$^+$ AML cells treated with vehicle or decitabine at 0.5 µM overnight in 3 independent replicates per condition.

Bisulfite conversion of isolated cell DNA was assessed using the Epitect Bisulfite Kit (QIAGEN) according to the manufacturer's protocol. The promoter region covering the binding sites for important transcription factors was selectively amplified using the following primers: forward 5′-GAGAGGGGTATACGAATATTTGG-3′; reverse 5′-ACCGCTACCAATCTAAAAATCC-3′. For the amplification of bisulfite-treated genomic DNA, the following PCR conditions were used: 1× 95 °C for 10 min; 40× 95 °C for 30 s; 56 °C for 30 s; 72 °C for 1 min; 1× 72 °C for 5 min. The PCR cocktail consisted of 3 µl of DNA (at least 10 ng µl^{-1} DNA for a final concentration of 3 ng µl^{-1} per reaction) in a 25 µl total volume using 1 µl of each primer (10 µM), 200 µM deoxynucleoside triphosphate, 0.2 U Hot Start Taq DNA polymerase, 2 µl Q-solution 5× (QIAGEN), 1.5 mM of $MgCl_2$ and the buffer supplied with the enzyme. Subsequent nested PCR was performed with the following primers: forward 5′-GAGTATTTTTAATTTTTGGATGTTTGTTG-3′; reverse 5′-ACAATTACCAAAATACAAACAATAACC-3′, using the same PCR conditions as described earlier for bisulfite sequencing. The amplified promoter region was gel-purified and subjected to fluorescent Sanger sequencing. The relative quantification of the methylated (C) versus unmethylated allele (T) was assessed using the QSVanalyzer software version 06-12-2012 (University of Leeds)[33].

Determination of synergy. Synergy between compounds was quantified using the Chou–Talalay method[22]. For the synergy studies, we calculated the percentage reduction of cell numbers after drug treatment compared to vehicle-treated cells. We determined the half maximal inhibitory concentration (IC_{50}) of cusatuzumab and decitabine in the presence of NK cells (derived from the buffy coats of healthy donors) and treated MOLM-13 cells with titrated concentrations of the compounds, below or above the IC_{50}. For the dose–effect analysis, the dose response values (IC_{50}), slope (m) and correlation coefficient (r) for the single treatments, as well as the combination index that reflects the extent of synergy or antagonism for two drugs were determined using the CompuSyn software version 1.0 (combination index < 1, synergy; combination index = 1, additivity; combination index > 1, antagonism).

scRNA-seq workflow and analysis. Barcoded cDNA from of at least 977 Lin$^-$CD34$^+$ cells from patients C8 and C10 was prepared using the Chromium Single Cell 3′ Library (v.2 Chemistry) & Gel Bead Kit on a Chromium Controller according to the manufacturer's recommendations (10x Genomics). The barcoded cDNA was further processed into scRNA-seq libraries and sequenced on a NovaSeq 6000 system using the NovaSeq Control Software v.1.6 (Illumina). Libraries were sequenced with 100 cycle S1 flow cell kits using the following paired-end configuration: 26 base pair (bp) Read 1; 91 bp Read 2.

To postprocess the samples and align the cDNA reads to the human reference transcriptome (GRCh38), we used the the CellRanger package v.2.1.1 (10x Genomics)[34]. This process allocates a unique molecular identifier (UMI, transcript) expression matrix to only those single cells containing a cell barcode (filtered feature barcode matrix). The expression matrix of each single cell was then normalized by the cellranger aggr function of the CellRanger package. This resulted in the identification of 4,883 cell barcodes with a median UMI per cell of 9,972 and median expression of 2,400 genes per cell for patient C8 and 2,266 cell barcodes with a median UMI per cell of 9,138 and median expression of 2,215 genes per cell for patient C10. Subsequently, the Seurat v.2.3.4 was used for quality control (filtering), graph-based clustering, visualization and differential gene expression analysis at the single-cell level[35]. Single cells identified by Seurat as outliers (>3,500 expressed genes) and cells showing a high level (>5%) of reads that aligned to the mitochondrial genome were removed[36]. To discriminate between malignant and healthy single cells in our samples, we took advantage of the molecular mutations identified at diagnosis in patients C8 and C10 and performed a data crushing approach. Single cells with a $\log_2$ gene expression $\geq 10^{-5}$ and $<10^{-5}$ of the respective marker(s) were considered as healthy cells and malignant cells, respectively. Unsupervised cell clustering and differential genes expression analysis of malignant cells for patients C8 and C10 at day −14 and C1D1 was performed using Seurat and its findMarker function, respectively. All figures and tables related to the scRNA-seq analysis were generated based on the filtered malignant cells.

Patients and study design. ARGX-110-1601 (NCT03030612) was a phase 1/2 open-label, dose-escalating study ($n = 12$ patients) with a proof of concept cohort ($n = 26$ patients) created to evaluate the safety, tolerability and efficacy of ARGX-110 in combination with azacitidine in individuals with newly diagnosed AML or high-risk myelodysplastic syndrome. This article reports the results of the dose escalation part of the phase 1/2 study ($n = 12$ patients). The dose escalation part used a 3+3 design to establish the maximum tolerated dose of cusatuzumab in combination with azacitidine. Cusatuzumab was administered intravenously every 2 weeks (first dose at day −14, all further applications on days 3 and 17 of all therapy cycles) at 1, 3, 10 and 20 mg kg^{-1} body weight in combination with standard doses of subcutaneous azacitidine of 75 mg m^{-2} given at days 1–7 every 28 d. The main inclusion criteria were: untreated AML ≥20% blasts; age ≥18 years; life expectancy ≥3 months; ECOG performance status of 0, 1 or 2. The main exclusion criteria were: previous or concurrent malignancy; any previous cancer chemotherapy or radiotherapy; abnormal organ function (aspartate aminotransferase and/or alanine aminotransferase >3× upper limit of normal (ULN) or in case of liver infiltration by AML, aspartate aminotransferase and/or alanine aminotransferase >5× ULN; alkaline phosphatase >2.5× ULN or in case of liver infiltration by AML, alkaline phosphatase >5× ULN; serum (total) bilirubin >1.5× ULN or in case of liver infiltration by AML, serum (total) bilirubin >5× ULN; serum creatinine >2.5× ULN or glomerular filtration rate (modification of diet in renal disease) of <40 ml min^{-1} for patients with creatinine levels above the normal limit); use of immunosuppressive agents for the previous 4 weeks. The primary objective of the phase 1 study was to determine the MTD of cusatuzumab (formerly ARGX-110) and/or the recommended phase 2 dose in combination with a standard dose of azacitidine. The secondary objectives involved evaluating the safety and tolerability, pharmacokinetics and immunogenicity, pharmacodynamics and preliminary efficacy of multiple ascending intravenous doses of cusatuzumab in combination with standard doses of azacitidine.

The trial (EudraCT no. 2016-002151-17) was sponsored by argenx and conducted in compliance with the Declaration of Helsinki (2013) and the International Conference on Harmonization Good Clinical Practices E6 (R2) Guidelines. The clinical study protocol and its amendments, informed consent documents and any other appropriate study-related documents were reviewed and approved by the applicable ethics committee in Bern and the national regulatory authority Swissmedic. Patients in the phase 1 trial were enrolled between January 2017 and March 2018 at the Inselspital, Bern University Hospital and University Hospital Zürich.

Samples were collected at diagnosis (day −14) and for the response assessment of cusatuzumab monotherapy (C1D1) at regular intervals during the trial. Pharmacodynamics and pharmacokinetics samples were collected during monotherapy and combination therapy. The intermediate cutoff for this report in the ongoing study was 18 February 2019.

Response criteria. The hematological remission status was assessed according to the criteria of the International Working Group[15,37]. MRD was evaluated by multiparameter flow cytometry according to the criteria of the ELN. The detection of at least 0.1% (>10^{-3}) of cells with a leukemia-associated immunophenotype was considered as a positive MRD result[38].

Cytogenetic and mutation analysis. Chromosome banding analysis from bone marrow was done according to standard procedures with a minimum of 20 metaphases required for a valid report. Fluorescence in situ hybridization and/or array comparative hybridization were added if needed for further clarification or to confirm the results of the chromosome banding analysis.

Mutations detected at diagnosis in the 12 patients in this study (for example, *CEBPA*, *EZH2*, *RUNX1*, *SH2B3*, *ZRSR2*, *NPM1*; see Supplementary Table 3) were determined by next-generation sequencing.

Statistical analysis. Statistical analysis was performed with Prism v.7.0. The bars and error bars indicate the means and s.d. unless otherwise specified in the figure legends. All statistical tests were two-sided and $P \leq 0.05$ (95% confidence interval) was considered statistically significant. Normality was measured using the D'Agostino–Pearson normality test for all experiments with $n \geq 8$. Correlations were performed using the Pearson correlation coefficient. Data were analyzed using a one-sample test (hypothetical value = 1); Student's t-test; paired t-test, one-way analysis of variance (ANOVA) followed by Tukey's multiple comparison test; and repeated measures one-way ANOVA followed by Tukey's multiple comparison test. The test applied to determine the statistical significance is specified in detail in the corresponding figure legend. LSC frequencies with 95% confidence intervals were estimated with the ELDA software and significant differences in LSC frequency were calculated by chi-squared test in limiting dilution assays according to Hu and Smyth[21]. The statistical analysis of differentially expressed genes in CD34$^+$ AML cells before and after cusatuzumab treatment was performed using a Wilcoxon rank-sum test followed by a Bonferroni-corrected P value.

Reporting Summary. Further information on research design is available in the Nature Research Reporting Summary linked to this article.

Data availability

The patient-related clinical datasets in the paper were generated during and analyzed as part of a multicenter clinical trial (NCT03030612). The datasets are not publicly available because the trial is ongoing, but data can be requested by any qualified researcher after data lock and trial completion or upon reasonable request. All RNA raw data and analyzed sequencing data can be retrieved from the Gene Expression Omnibus and are available under accession no. GSE147989 (scRNA-seq). All other data that support the findings of the study are available from the corresponding authors upon request.

Code availability

The code used for the analysis of the single-cell sequencing data is available from the corresponding author upon request.

References

29. Harris, P. A. et al. Research electronic data capture (REDCap)—a metadata-driven methodology and workflow process for providing translational research informatics support. *J. Biomed. Inform.* **42**, 377–381 (2009).
30. Murone, M. et al. The multi-kinase inhibitor Debio 0617B reduces maintenance and self-renewal of primary human AML $CD34^+$ stem/progenitor cells. *Mol. Cancer Ther.* **16**, 1497–1510 (2017).
31. Wang, J. C. Y. & Dick, J. E. Cancer stem cells: lessons from leukemia. *Trends Cell Biol.* **15**, 494–501 (2005).
32. Majeti, R. et al. CD47 Is an adverse prognostic factor and therapeutic antibody target on human acute myeloid leukemia stem cells. *Cell* **138**, 286–299 (2009).
33. Carr, I. M. et al. Inferring relative proportions of DNA variants from sequencing electropherograms. *Bioinformatics* **25**, 3244–3250 (2009).
34. Dobin, A. et al. STAR: ultrafast universal RNA-seq aligner. *Bioinformatics* **29**, 15–21 (2013).
35. Butler, A., Hoffman, P., Smibert, P., Papalexi, E. & Satija, R. Integrating single-cell transcriptomic data across different conditions, technologies, and species. *Nat. Biotechnol.* **36**, 411–420 (2018).
36. Ilicic, T. et al. Classification of low quality cells from single-cell RNA-seq data. *Genome Biol.* **17**, 29 (2016).
37. Cheson, B. D. et al. Revised recommendations of the international working group for diagnosis, standardization of response criteria, treatment outcomes, and reporting standards for therapeutic trials in acute myeloid leukemia. *J. Clin. Oncol.* **21**, 4642–4649 (2003).
38. Schuurhuis, G. J. et al. Minimal/measurable residual disease in AML: a consensus document from the European LeukemiaNet MRD working party. *Blood* **131**, 1275–1291 (2018).

Acknowledgements

We thank U. Lüthi and T. Chiorazzo for providing excellent technical assistance; the FACSlab of the Department for BioMedical Research for assistance with cell sorting; the Next Generation Sequencing Platform of the University of Bern for performing the high-throughput sequencing experiments; and the Interfaculty Bioinformatics Unit of the University of Bern for providing the high-performance computing infrastructure. We especially thank the teams of the Clinical Research Unit of the Department of Medical Oncology, Bern University Hospital and University Hospital Zürich, the University of Zürich and the histopathology laboratory at the Institute of Pathology, Bern. In addition, we thank B. Lambrecht from Ghent University for helpful discussions during the preparation of the manuscript. The preclinical work was supported by grants from the Swiss National Science Foundation (nos. 31003A_149768 and 310030B_13313 to A.F.O., and 310030_179394 to C.R.), the Swiss Cancer League (no. KLS-3346-02-2014), the Sassella Foundation, the Fondazione Dr. Carlo Gianella, the Wolfermann-Nägeli Foundation, the Olga Mayenfisch Foundation, Alfred und Anneliese Sutter-Stöttner Foundation and the Fondazione per la Ricerca sulla Trasfusione e sui Trapianti (to C.R.). The clinical study was financed by argenx. The translational work was supported by the SAKK/Gateway/Rising Tide Foundation (to A.F.O).

Author contributions

C.R. and A.F.O. conceived and designed the preclinical and translational experiments. A.F.O., T.P., U.B., S.F., N.L., E.E., D.G., L.V.R. and H.D.H. conceived and designed the clinical trial. A.F.O., T.P., R.M. and M.G.M. selected and treated the patients. C.R., T.P., S.H., U.B., Y.B., M.H., R.M., L.V.R., A.H., M.M., T.D., D.G., E.E., W.H.G., D.F., R.B. and N.L. collected and assembled the data. C.R., T.P., S.H., U.B., Y.B., M.H., A.F.O., W.H.G., D.F., R.B., L.V.R., A.H., M.M., T.D., D.G., E.E., H.D.H. and N.L. analyzed and interpreted the data. C.R., T.P., U.B., A.F.O., A.H., H.D.H. and N.L. wrote the manuscripts. All authors revised the manuscript and approved its final version.

Competing interests

C.R. and A.F.O. are listed as investors on a patent held by the University of Bern on targeting CD70 for the treatment of AML. M.M., T.D., N.L., E.E., D.G., L.V.R., A.H. and H.D.H are employees of argenx. S.F. is a consultant for argenx. All other authors declare no competing interests related to the current study.

Additional information

Supplementary information is available for this paper at https://doi.org/10.1038/s41591-020-0910-8.

Correspondence and requests for materials should be addressed to C.R. or A.F.O.

Peer review information Javier Carmona was the primary editor on this article and managed its editorial process and peer review in collaboration with the rest of the editorial team.

nature research

Corresponding author(s): Carsten Riether
Adrian F. Ochsenbein

Last updated by author(s): April 15, 2020

Reporting Summary

Nature Research wishes to improve the reproducibility of the work that we publish. This form provides structure for consistency and transparency in reporting. For further information on Nature Research policies, see Authors & Referees and the Editorial Policy Checklist.

Statistics

For all statistical analyses, confirm that the following items are present in the figure legend, table legend, main text, or Methods section.

n/a	Confirmed	
☐	☒	The exact sample size (*n*) for each experimental group/condition, given as a discrete number and unit of measurement
☐	☒	A statement on whether measurements were taken from distinct samples or whether the same sample was measured repeatedly
☐	☒	The statistical test(s) used AND whether they are one- or two-sided *Only common tests should be described solely by name; describe more complex techniques in the Methods section.*
☒	☐	A description of all covariates tested
☐	☒	A description of any assumptions or corrections, such as tests of normality and adjustment for multiple comparisons
☐	☒	A full description of the statistical parameters including central tendency (e.g. means) or other basic estimates (e.g. regression coefficient) AND variation (e.g. standard deviation) or associated estimates of uncertainty (e.g. confidence intervals)
☒	☐	For null hypothesis testing, the test statistic (e.g. *F*, *t*, *r*) with confidence intervals, effect sizes, degrees of freedom and *P* value noted *Give P values as exact values whenever suitable.*
☒	☐	For Bayesian analysis, information on the choice of priors and Markov chain Monte Carlo settings
☒	☐	For hierarchical and complex designs, identification of the appropriate level for tests and full reporting of outcomes
☐	☒	Estimates of effect sizes (e.g. Cohen's *d*, Pearson's *r*), indicating how they were calculated

Our web collection on statistics for biologists contains articles on many of the points above.

Software and code

Policy information about availability of computer code

Data collection	The barcoded cDNA was sequenced on a NovaSeq 6000 instrument using NovaSeq Control Software v1.6 (Illumina). FACS samples were acquired on BD FACS Fortessa using FACS DIVA software. FACS sorting was performed on a FACS Aria III. Study data were collected and managed using REDCap electronic data capture tools. qRT-PCR reactions were performed in duplicates including non-template controls
Data analysis	ELDA: http://bioinf.wehi.edu.au/software/elda/; CellRanger package (v2.1.1), Seurat package (v2.3.4); CompuSyn software: http://www.combosyn.com/.sing an ABI Prism 7500 Sequence Detection System (Applied Biosystems). FACS: FACS DIVA software and FlowJo software . Statistics. GraphPad Prism. Methylation: QSVAnalyser software. The code used for the analysis of the single cell sequencing data are available from the corresponding author upon request.

Data

Policy information about availability of data

All manuscripts must include a data availability statement. This statement should provide the following information, where applicable:

- Accession codes, unique identifiers, or web links for publicly available datasets
- A list of figures that have associated raw data
- A description of any restrictions on data availability

Data availability statement
Patient-related clinical data sets in the paper were generated during and analyzed as part of the part of a multicenter clinical trial (NCT03030612). The data sets are not publicly available because the trial is still ongoing, but data can be requested by any qualified researcher after data lock and completion of trial or on reasonable request.
All RNA raw data, the analyzed sequencing data can be found at the GEO database and are available via accession number GSE147989 (single cell RNA-seq).
All other data that support the findings of the study are available from the corresponding author upon request.

Code availability statement
The code used for the analysis of the single cell sequencing data are available from the corresponding author upon request.

Field-specific reporting

Please select the one below that is the best fit for your research. If you are not sure, read the appropriate sections before making your selection.

☒ Life sciences ☐ Behavioural & social sciences ☐ Ecological, evolutionary & environmental sciences

For a reference copy of the document with all sections, see nature.com/documents/nr-reporting-summary-flat.pdf

Life sciences study design

All studies must disclose on these points even when the disclosure is negative.

Sample size	No sample size was used for the pre-clinical experiments. Samples numbers were determined based on the availability of primary material Transaltional experiments were performed based on sample availability. The dose escalation part of the clinical trial was performed in a classical 3+3 design.
Data exclusions	Single cell RNA sequencing: Single cells identified by the Seurat package as outliers (>3500 expressed genes) and cells that showed a high level (>5%) of reads that aligned to the mitochondrial genome were removed from the analysis
Replication	As the vast majority of the experiments were performed with primary human patient samples, experiments could not be repeated due to limited patient material. This caveat was overcome by the analysis of different patient samples in the different assays.
Randomization	Randomization of mice into treatment group was performed using GraphPad software random number generator.
Blinding	Experiments were conducted and analyzed in a non-blinded fashion. Blinding was not relevant to the preclinical study because resultd were tested further in a clinical study. The clinical study was not blinded because it had just one treatment arm.

Reporting for specific materials, systems and methods

We require information from authors about some types of materials, experimental systems and methods used in many studies. Here, indicate whether each material, system or method listed is relevant to your study. If you are not sure if a list item applies to your research, read the appropriate section before selecting a response.

Materials & experimental systems

n/a	Involved in the study
☐	☒ Antibodies
☒	☐ Eukaryotic cell lines
☒	☐ Palaeontology
☐	☒ Animals and other organisms
☐	☒ Human research participants
☐	☒ Clinical data

Methods

n/a	Involved in the study
☒	☐ ChIP-seq
☐	☒ Flow cytometry
☒	☐ MRI-based neuroimaging

Antibodies

Antibodies used	CD34-APC (cat. 343607, clone 561, 1:80), CD34-PE (cat. 343603, clone 561, 1:100), CD38-PE-Cy7 (cat. 303515, clone HIT2, 1:50), CD90-PerCP-Cy5.5 (cat. 382113, clone 5E10, 1:100), CD33-PerCP-Cy5.5 (cat 302413, clone WM53, 1:100), CD45RA-APC-Cy7 (cat. 304151, clone HI100, 1:20), CD8a-PerCP-Cy5.5 (cat. 300923, clone HIT8a, 1:100), CD4-PerCP-Cy5.5 (cat. 344607, clone SK3, 1:100), CD19-APC-Cy7 (cat 302217, clone HIB19, 1:100), mouse- CD45-PerCP-Cy5.5 (cat. 103131, clone 30-F11, 1:200), mouse- CD45-PE-Cy7 (cat. 103113, clone 30-F11, 1:200), Annexin-V-Pacific blue (1:50) were from BioLegend. Lineage-positive cells were excluded by staining using biotinylated CD2 (cat. 300203, clone RPA2.10, 1:100), CD3 (cat. 317319, clone OKT3, 1:100), aCD14 (cat. 325623, clone HCD14, 1:100), CD16 (cat. 302003, clone 3G8, 1:100), CD19 (cat. 302203, clone HIB19, 1:100), CD56 (cat. 318319, clone HCD56, 1:100) and CD235 (cat. 306617, clone HIR2, 1:100) (BioLegend), followed by a second step using streptavidin-FITC (BD Pharmingen, 1:3000). CD70-PE (cat. 555835, clone KI-24, 1:10) and corresponding isotype control mAb were from BD Pharmingen. Viability dye eFluor450 was from eBioscience (1:1000). CD45 V500C (cat. 56077; clone 2DI, 1:50) was from BD Pharmingen.
Validation	All antibodies were titrated and validated on primary mouse or human cells using a positive and negative control based on the description on the datasheet of the manufacturer.

Eukaryotic cell lines

Policy information about cell lines

Cell line source(s)	MOLM-13 and MONO-1 cells were specifically purchased from ATCC for this study. Therefore, the authors performed no additional authentication.
Authentication	
Mycoplasma contamination	The cell line was tested mycoplasma-free
Commonly misidentified lines (See ICLAC register)	Human cell lines employed were either not listed in the cross-contaminated or misidentified cell lines database curated by the International Cell Line Authentication Committee (ICLAC)

Animals and other organisms

Policy information about studies involving animals; ARRIVE guidelines recommended for reporting animal research

Laboratory animals	NOD/LtSz-scid IL2Rgnull (NSG) mice were purchased from Charles River (Sulzfeld, Germany). 6-8 weeks old male and female mice

Laboratory animals	were housed under specific pathogen-free conditions in individually ventilated cages with food and water ad libitum and were regularly monitored for pathogens. All animals used in the experiments were age- and sex-matched.
Wild animals	Study did not involve wild animals.
Field-collected samples	Study did not involve field-collected samples.
Ethics oversight	Experiments were approved by the local experimental animal committee of the Canton of Bern and performed according to Swiss laws for animal protection (BE75/17 and BE78/17).

Note that full information on the approval of the study protocol must also be provided in the manuscript.

Human research participants

Policy information about studies involving human research participants

Population characteristics	Patients enrolled in the clinical study were all above age 64 (range 65-84 years, 5 x male and 3 x female) and were newly diagnosed for AML.
Recruitment	Patients fulfilling the specified inclusion / exclusion criteria (see study protocol) were recruited at the University Hospital Bern, University Hospital Zurich and in the Kantonal Hospital Aarau between 1/2017 and 3/2018. No other selection criteria except the defined inclusion / exclusion criteria have been used. Patients were recruited consecutivley based on restrictions and saftety assessement by the local ethical commitee.
Ethics oversight	The clinical study protocol and its amendments, informed consent documents, and any other appropriate study-related documents were reviewed and approved by the applicable ethics committee of Bern, Switzerland, and the national regulatory authorities Swissmedic in Bern, Switzerland.

Note that full information on the approval of the study protocol must also be provided in the manuscript.

Clinical data

Policy information about clinical studies

All manuscripts should comply with the ICMJE guidelines for publication of clinical research and a completed CONSORT checklist must be included with all submissions.

Clinical trial registration	NCT03030612
Study protocol	Provided with the submission documents
Data collection	Patients in the phase 1 part of the trial were enrolled between January 2017 and March 2018 at the Inselspital, Bern University Hospital and the University Hospital Zürich. The intermediate cut-off for this report in the ongoing study was October 15 2018.
Outcomes	The primary objective of the phase 1 was to determine the MTD of cusatuzumab (formerly ARGX-110) and/or the recommended phase 2 dose (RP2D) in combination with a standard dose of azacitidine. The secondary objectives involved evaluating the safety and tolerability, the pharmacokinetics and immunogenicity, the pharmacodynamics and preliminary efficacy of multiple ascending intravenous doses of cusatuzumab in combination with standard doses of azacitidine.

ChIP-seq

Data deposition

☐ Confirm that both raw and final processed data have been deposited in a public database such as GEO.

☐ Confirm that you have deposited or provided access to graph files (e.g. BED files) for the called peaks.

Data access links *May remain private before publication.*	*For "Initial submission" or "Revised version" documents, provide reviewer access links. For your "Final submission" document, provide a link to the deposited data.*
Files in database submission	*Provide a list of all files available in the database submission.*
Genome browser session (e.g. UCSC)	*Provide a link to an anonymized genome browser session for "Initial submission" and "Revised version" documents only, to enable peer review. Write "no longer applicable" for "Final submission" documents.*

Methodology

Replicates	*Describe the experimental replicates, specifying number, type and replicate agreement.*
Sequencing depth	*Describe the sequencing depth for each experiment, providing the total number of reads, uniquely mapped reads, length of reads and whether they were paired- or single-end.*
Antibodies	*Describe the antibodies used for the ChIP-seq experiments; as applicable, provide supplier name, catalog number, clone name, and lot number.*

Peak calling parameters	*Specify the command line program and parameters used for read mapping and peak calling, including the ChIP, control and index files used.*
Data quality	*Describe the methods used to ensure data quality in full detail, including how many peaks are at FDR 5% and above 5-fold enrichment.*
Software	*Describe the software used to collect and analyze the ChIP-seq data. For custom code that has been deposited into a community repository, provide accession details.*

Flow Cytometry

Plots

Confirm that:

☒ The axis labels state the marker and fluorochrome used (e.g. CD4-FITC).

☒ The axis scales are clearly visible. Include numbers along axes only for bottom left plot of group (a 'group' is an analysis of identical markers).

☐ All plots are contour plots with outliers or pseudocolor plots.

☒ A numerical value for number of cells or percentage (with statistics) is provided.

Methodology

Sample preparation	Flow cytometric analysis on whole BM was performed following red blood cell (RBC) lysis.
Instrument	Samples were analyzed on a BD Fortessa and sorting procedures were performed using a BD FACS Aria III (BD Biosciences).
Software	Data were collected using FACSDiva software (BD Pharmingen) analyzed using FlowJo software (Treestar).
Cell population abundance	Effective separation after FACS-sorting was assessed by re-analyzing a fraction of the sorted samples by flow-cytometry analysis.
Gating strategy	Gating strategies for all relevant experiments are depicted in the manuscript.

☒ Tick this box to confirm that a figure exemplifying the gating strategy is provided in the Supplementary Information.

Magnetic resonance imaging

Experimental design

Design type	*Indicate task or resting state; event-related or block design.*
Design specifications	*Specify the number of blocks, trials or experimental units per session and/or subject, and specify the length of each trial or block (if trials are blocked) and interval between trials.*
Behavioral performance measures	*State number and/or type of variables recorded (e.g. correct button press, response time) and what statistics were used to establish that the subjects were performing the task as expected (e.g. mean, range, and/or standard deviation across subjects).*

Acquisition

Imaging type(s)	*Specify: functional, structural, diffusion, perfusion.*
Field strength	*Specify in Tesla*
Sequence & imaging parameters	*Specify the pulse sequence type (gradient echo, spin echo, etc.), imaging type (EPI, spiral, etc.), field of view, matrix size, slice thickness, orientation and TE/TR/flip angle.*
Area of acquisition	*State whether a whole brain scan was used OR define the area of acquisition, describing how the region was determined.*

Diffusion MRI ☐ Used ☐ Not used

Preprocessing

Preprocessing software	*Provide detail on software version and revision number and on specific parameters (model/functions, brain extraction, segmentation, smoothing kernel size, etc.).*
Normalization	*If data were normalized/standardized, describe the approach(es): specify linear or non-linear and define image types used for transformation OR indicate that data were not normalized and explain rationale for lack of normalization.*

Normalization template

Describe the template used for normalization/transformation, specifying subject space or group standardized space (e.g. original Talairach, MNI305, ICBM152) OR indicate that the data were not normalized.

Noise and artifact removal

Describe your procedure(s) for artifact and structured noise removal, specifying motion parameters, tissue signals and physiological signals (heart rate, respiration).

Volume censoring

Define your software and/or method and criteria for volume censoring, and state the extent of such censoring.

Statistical modeling & inference

Model type and settings

Specify type (mass univariate, multivariate, RSA, predictive, etc.) and describe essential details of the model at the first and second levels (e.g. fixed, random or mixed effects; drift or auto-correlation).

Effect(s) tested

Define precise effect in terms of the task or stimulus conditions instead of psychological concepts and indicate whether ANOVA or factorial designs were used.

Specify type of analysis: ☐ Whole brain ☐ ROI-based ☐ Both

Statistic type for inference
(See Eklund et al. 2016)

Specify voxel-wise or cluster-wise and report all relevant parameters for cluster-wise methods.

Correction

Describe the type of correction and how it is obtained for multiple comparisons (e.g. FWE, FDR, permutation or Monte Carlo).

Models & analysis

n/a	Involved in the study
☒	☐ Functional and/or effective connectivity
☒	☐ Graph analysis
☒	☐ Multivariate modeling or predictive analysis